Probabilistic planning of a battery energy storage system in a hybrid microgrid based on the Taguchi arrays

Electrical Power and Energy Systems 157 (2024) 109886

Contents lists available at ScienceDirect

International Journal of Electrical Power and Energy Systems

journal homepage: www.elsevier.com/locate/ijepes

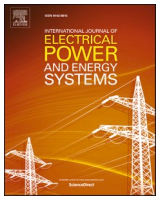

Probabilistic planning of a battery energy storage system in a hybrid microgrid based on the Taguchi arrays

Fabio Mottola [a,*], Daniela Proto [a], Angela Russo [b]

[a] University of Naples Federico II, Department of Electrical Engineering and Information Technology, Via Claudio, 21, 80125 Naples, Italy
[b] Politecnico di Torino, Energy Department, Corso Duca Degli Abruzzi, 24, 10129 Torino, Italy

ARTICLE INFO

Keywords:
Battery energy storage system
Probabilistic sizing
Taguchi arrays

ABSTRACT

The transformation of electrical networks in the context of the new smart grid paradigm unavoidably involves new challenges for electrical component planning. This paper provides a tool for the probabilistic sizing of a battery energy storage system in a hybrid AC/DC microgrid (i.e., a microgrid including AC and DC subsections with AC and DC loads and renewable power generation). The procedure is based on an analytical formulation to assess the total costs sustained by the microgrid for the inclusion of the battery energy storage system. The total costs depend on the random nature of the load demand, the electrical energy prices, and the renewable power generation, therefore, a probabilistic approach has been used. Furthermore, to account for uncertainties that affect the input data, the Taguchi orthogonal arrays are applied which allow significantly reducing the computational efforts while guaranteeing the desired accuracy of the results. The proposed analytical formulation along with the use of the Taguchi orthogonal arrays allows limiting the computational complexity even in presence of a large number of random inputs and discretization levels. A case study based on an industrial hybrid microgrid is presented to analyse the results obtained in terms of the optimal sizing of the battery energy storage system and to investigate the sensitivity with respect to some inputs.

1. Introduction

Battery energy storage systems (BESSs) are recognized to be essential in the path towards the effective integration of renewable energy in microgrids (μGs). The advantages of the BESS deployment are numerous and range from the simple ability to store the energy when it is in excess and use it as it is needed to the achievement of economic and sustainable goals in the operation of the electrical grids [1].

The proper installation of a BESS in a μG is driven by both economic and technical considerations. Indeed, the investment costs, which decreased over the last years, still represent an important item of the total costs; moreover, the O&M costs are linked to the strategy of the charging/discharging of storage systems. Such that, the optimal sizing of a BESS has to be faced as a constrained optimization problem [1].

The BESS sizing is an optimization problem that involves a long period (multiple years) so that uncertainties of the input variables cannot be neglected and have to be carefully considered [1,2]. Indeed, long-term and short-term uncertainties can be recognized; the former mainly refer to the load growth and the electrical energy tariffs; the latter are mainly linked to load and renewable generation variations. Both have to be correctly addressed as random variables in order to obtain a sizing which proves to be adequate and performing over the planning period. Therefore, the best approach for BESS sizing is based on the formulation of a probabilistic optimization problem.

1.1. Probabilistic sizing of storage systems - literature review

Several contributions are available in the relevant literature addressing the probabilistic sizing of storage systems [2–18]. They differ according to the objectives of the sizing, the typologies and the characterization of uncertainties, and the methods used for solving the probabilistic sizing problem.

Indeed, the probabilistic sizing of BESSs can be adopted by pursuing different objectives. A frequent objective is of economic nature; [3,4], and [18] choose the size of the BESS that minimizes the total costs including the BESS installation and operation cost and the cost of the energy exchanged with the grid. The economic value of load curtailment [5] and of the reliability [6,7] can also be included in the cost function. A technical objective is considered in [8] related to over- and under-voltage while the improvement of the self-consumption of renewable

* Corresponding author.
E-mail addresses: fabio.mottola@unina.it (F. Mottola), daniela.proto@unina.it (D. Proto), angela.russo@polito.it (A. Russo).

https://doi.org/10.1016/j.ijepes.2024.109886
Received 11 May 2023; Received in revised form 24 January 2024; Accepted 19 February 2024

generation is attained in [9]. When BESSs are installed in coordination with renewable generators, they can help reduce the detrimental effect of forecast errors of renewable generation [10–14].

The probabilistic approaches for BESS sizing consider different uncertainties [3,4,6–9,15,16,18]: load demand, electricity prices (both intended as tariffs and selling price), photovoltaic (PV) and wind generation are the most frequently treated.

Different probabilistic methods have been applied to consider the above objectives and uncertainties. In addition to the common procedure based on the time-consuming Monte Carlo simulation characterized by a significant number of trials [3,9,12], many authors tried to limit the computational burden by applying the Point- Estimate method [6,7,14], the Chance-Constrained based method [15,17], the scenario-based approach [2,4,5,8] and the static robust optimization [16].

1.2. Contributions and organization of the paper

The paper focuses on a particular application which refers to the case of a hybrid μG including AC and DC loads, renewable energy source (RES) power generation and a storage device. The μG, which is connected to an upstream grid through a point of common coupling, also includes a DC bus where the DC loads, the PV generation and the storage are connected.

Starting from this configuration, in this paper, the optimal sizing problem of the BESS is carried out by minimizing a closed form of the total costs and is faced by considering uncertainties in load demand, electrical energy prices, and RES power generation. An analytical formulation is provided allowing determining the total costs given by the cost sustained for the purchased energy and the profit derived from the sold energy, both referred to the whole planning period, and the BESS's installation and operation costs. In particular, the closed-form analytical expression of the total cost considers the adopted energy management strategy of the μG to control the balance among the loads, the photovoltaic power production, the BESS power, and the power exchanged with the main grid.

The probabilistic approach used in this paper makes use of the Taguchi arrays-based method [19] whose advantage in this application is mainly related to its ability to obtain the mean values of the total costs with a few numbers of trials on the input random variables. This allows guaranteeing very reduced computational complexity with high accuracy of the results. The probabilistic approach, indeed, could imply a high computational effort especially when dealing with a very high number of both random inputs and discretization levels and when the use of the Monte Carlo approach would require a very high number of experiments to provide accurate results. In these cases, the combination of closed-form relationships and the Taguchi method offers accurate and fast solutions. The Taguchi arrays-based method has been used extensively in various fields of engineering, but only recently it has been used in the field of power systems [20–33] and never applied, to the best of our knowledge, to the probabilistic BESS sizing.

The main contributions of this paper are summarized as follows:

(i) an analytical formulation of the total costs in a μG including a BESS, AC and DC loads and renewable generation is provided; this formulation can be easily applied in the probabilistic framework of the BESS design, limiting the computational efforts;
(ii) a probabilistic solving procedure of the BESS sizing based on the Taguchi arrays is applied; the innovative proposed procedure allows obtaining the BESS design parameters with reduced computational burden;
(iii) a comparison of the computational efforts and the accuracy of the results of the proposed approach with those associated with the classical Monte Carlo simulation procedure is carried out. Also, a wide sensitivity analysis is conducted to assess the influence of the main input parameters.

The paper is organized as follows. Section 2 presents the proposed procedure adopted for solving the probabilistic sizing of a BESS in a μG. Section 3 provides the evaluation of the total costs sustained for the installation/maintenance of the BESS and the exchange of electrical energy with the upstream grid while Section 4 describes the energy management strategy of the μG and the charging/discharging process of the BESS. The application of Taguchi's arrays to the sizing problem under consideration is derived in Section 5. Finally, numerical results are illustrated and discussed in Section 6 and conclusions are drawn in Section 7.

2. The probabilistic sizing procedure

The proposed sizing procedure is based on a probabilistic procedure for sizing BESSs included in hybrid AC-DC μGs [34] whose conceptual scheme is that shown in Fig. 1. For this purpose, an analytical formulation of the total cost is derived including the cost sustained for the purchased energy and the profit derived from the sold energy, both referred to the whole planning period, as well as the BESS's installation and operation costs. The analytical formulation of the total cost is then used in the probabilistic method which provides the expected mean value of the total cost related to the uncertainties affecting some input parameters.

In particular, the BESS sizing random input variables refer to economic aspects, e.g., price of sold/purchased energy, and technical aspects that are load demand and RES power. The Taguchi arrays-based probabilistic procedure is repeatedly applied to several BESS sizes and the optimal size is chosen as that corresponding to the minimum value of

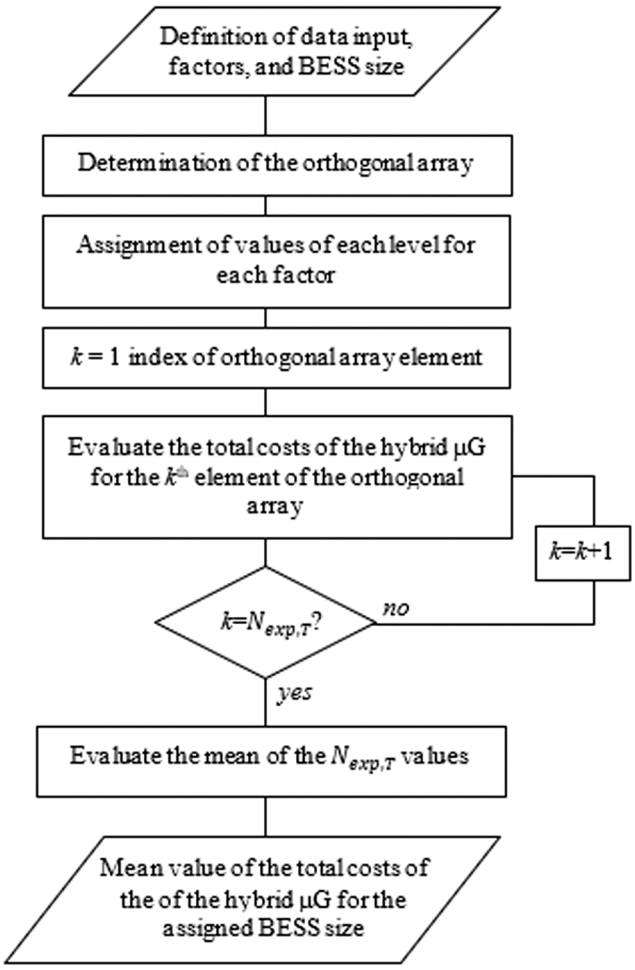

Fig. 1. Scheme of the typology of hybrid μG considered.

the expected total cost.

More in detail, the proposed probabilistic sizing procedure includes the following steps:

- input of the data needed for the cost evaluation formulated in terms of probability density functions (pdfs);
- evaluation of the mean value of the cost for each considered BESS size;
- identification of the BESS size as that corresponding to the minimum cost.

A schematic of the procedure is reported in Fig. 2.

Pre-processing of input data has to be carried out consisting of data cleansing, averaging, and clustering. Regarding data cleansing, bad and missing data have to be individuated and removed. With reference to the averaging, all the values have to be averaged at the same time resolution.

The clustering of data refers to the identification of typical days that are characterized by similar profiles of the inputs based on their seasonality.

The cost evaluation is based on the analytical formulation presented in Sections 3 and 4. This formulation is iteratively applied to all the candidate BESS sizes (N_{bs}) and, for each of them, the mean values of the cost are determined through the Taguchi-based probabilistic procedure whose details are given in Section 5. The optimal BESS is finally derived as that corresponding to the minimum cost mean value.

3. Cost evaluation

The cost sustained by the μG reported in Fig. 1 is formulated in terms of total cost function, C_T, related to the inclusion of the BESS in the μG

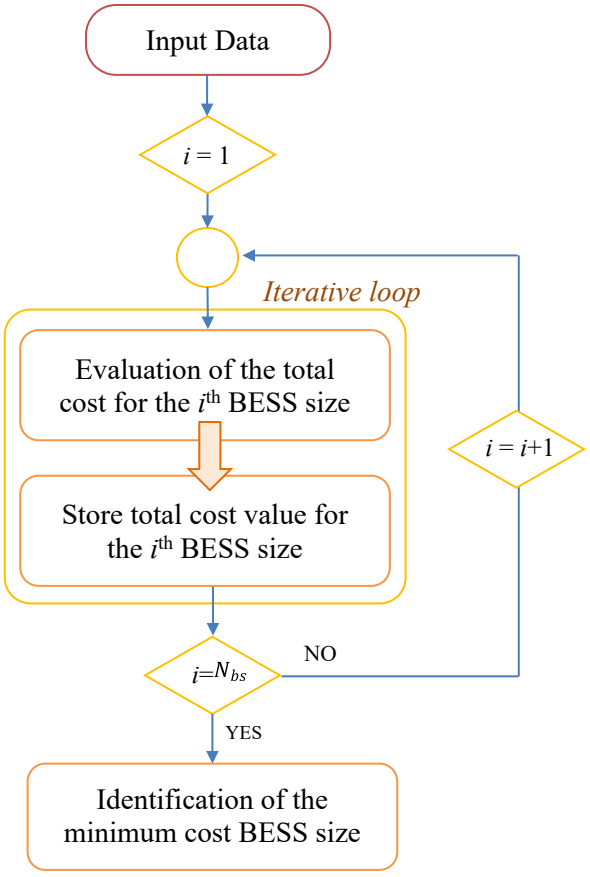

Fig. 2. Flowchart of the sizing procedure.

which is defined as:

$$C_T = C_0 + C_M + C_R + C_D + C_E - R_E \tag{1}$$

where C_0 includes the BESS installation cost, C_M is the battery maintenance cost, C_R is the cost related to the replacement of the battery, C_D is the cost of the disposal of the battery, C_E is the cost sustained due to the energy purchased by the μG, and R_E is the revenue for the energy sold by the μG. The energy purchased from the network and that sold to the network include the whole energy exchanged by the hybrid μG, thus comprising that of loads, RES, and BESS.

Regarding the cost related to the replacement of the battery, the expected lifetime of the battery has to be evaluated by taking into account its life cycle that is the total number of charging/discharging cycles corresponding to a specific battery technology and a maximum Depth of Discharge (DoD). The battery lifetime is then given by: $L_b = \frac{N_{cycles}(DoD)}{365\upsilon}$, where L_b is the battery lifetime (in years), $N_{cycles}(DoD)$ is the total number of charging/discharging cycles corresponding to a specific maximum DoD, being this value declared by the battery manufacturer, and υ is the number of daily charging/discharging cycles, that depends on how the battery is operated.

The cost items C_E and R_E in (1) are related to the whole planning period (N_{years}) of the BESS as:

$$C_E = \sum_{n=1}^{N} \frac{\sum_{k=1}^{Sn} D(k) C_{E,n,k}}{(1+\beta)^{n-1}} \tag{2}$$

$$R_E = \sum_{n=1}^{N} \frac{\sum_{k=1}^{Sn} D(k) R_{E,n,k}}{(1+\beta)^{n-1}} \tag{3}$$

with β the discount rate and Sn the time periods of each year (e.g., seasons), each characterized by a typical day repeated $D(k)$ times per year; with respect to the typical day of the kth time period of the nth year, $C_{E,n,k}$ is the cost sustained for the purchased energy, and $R_{E,n,k}$ is the revenue for the sold energy. Both these last terms depend on the price of the energy. In the case of the ToU tariff, different price levels (typically, two or three) are defined, each corresponding to specified periods (hours) of the day. In the case of two price levels (it is easy to extend to the case of more levels), that is on-peak and off-peak periods, $C_{E,n,k}$ and $R_{E,n,k}$ can be defined as:

$$C_{E,n,k} = E_{n,k}^{p,T^{on}} \mathrm{Pr}_{\mathrm{n,k}}^{\mathrm{on}} + E_{n,k}^{p,T^{off}} \mathrm{Pr}_{\mathrm{n,k}}^{\mathrm{off}} \tag{4}$$

$$R_{E,n,k} = E_{n,k}^{s,T^{on}} \mathrm{Pr}_{\mathrm{n,k}}^{\mathrm{f}} + E_{n,k}^{s,T^{off}} \mathrm{Pr}_{\mathrm{n,k}}^{\mathrm{f}} \tag{5}$$

where $E_{n,k}^{p,T^{on}}$ ($E_{n,k}^{p,T^{off}}$) and $E_{n,k}^{s,T^{on}}$ ($E_{n,k}^{s,T^{off}}$) are the energy purchased from the grid during the on-peak (off-peak) periods, and the energy sold to the grid during the on-peak (off-peak) periods, respectively. $\mathrm{Pr}_{\mathrm{n,k}}^{\mathrm{on}}$ and $\mathrm{Pr}_{\mathrm{n,k}}^{\mathrm{off}}$ are the prices of the energy purchased from the grid during these periods and $\mathrm{Pr}_{\mathrm{n,k}}^{\mathrm{f}}$ is the price of the feed-in tariff for the energy sold. The values of the sold and purchased energy in (4) and (5) depend on the energy management strategy of the μG and, in particular, of the storage system. In the next Section, this strategy is discussed and the formulae for the evaluation of $E_{n,k}^{p,T^{on}}$, $E_{n,k}^{p,T^{off}}$, $E_{n,k}^{s,T^{on}}$, and $E_{n,k}^{s,T^{off}}$ are derived in closed form.

4. Energy management and energy exchanges

The energy management strategy of the μG aims to control the balance among the loads, the RES power production, the BESS power, and the power exchanged with the main grid. The proposed strategy is pursued by controlling the battery charging/discharging power to minimize the daily cost related to the power absorbed (purchased) from the main grid and to maximize the revenue related to the power

exported (sold) to the grid. For this purpose, in the case of ToU tariffs, the management strategy has to be hierarchically arranged to allow:

- the use of RES power to supply the DC load, first, then the AC load during all periods of the day;
- the BESS discharging to supply loads exceeding the RES power production, during the on-peak time period;
- the BESS charging being supplied by the RES exceeding the loads, and that supplied by the grid, during the off-peak time period;
- the export to the main grid of the RES production exceeding the sum of load and battery powers.

With respect to the charged/discharged energy of the BESS, the proposed energy management strategy is schematized in Fig. 3, where the term "load" refers to the sum of DC and AC loads.

It has to be noted that the proposed strategy is particularly tailored for systems in which the RES size is not big enough to satisfy the load demand, especially in winter and mid-season. Also, the main purpose of the strategy is the provision of demand response rather than the increase in self-consumption.

The application of this strategy is subject to the constraints related to (i) the battery rating and DoD, (ii) the contractual agreement in terms of the maximum value of power exchanges between the μG and the grid, and (iii) the daily energy balance. These constraints mean that the areas reported in Fig. 3 (areas from ① to ⑥) refer to the maximum energy available for discharging, e^{dch}_{max}, (i.e., areas ② and ③) or charging, e^{ch}_{max}, (i.e., areas ⑤, and ⑥). The maximum energy available for charging (area ⑥) is related to the limits imposed on the power that can be imported from the main grid and the area ① refers to the energy produced by the RES and exported to the main grid.

The proposed analytical approach is then based on the comparison between the daily profiles of load demand and power production. Based on this comparison, the maximum energy the battery can charge, e^{ch}_{max}, and the maximum energy the battery can discharge, e^{dch}_{max}, are evaluated. On a daily basis, it is required that the charged and discharged energy be the same; these values are also limited by the maximum energy the battery can store s, which accounts for the size and the maximum DoD. Then, the value of the daily energy the battery can charge, or discharge, e, is given by (hereinafter, the indices n and k are not considered for ease of notation):

$$e = min\left\{e^{ch}_{max}, e^{dch}_{max}, s\right\} \tag{6}$$

The maximum energy that can be discharged/charged by the BESS is analytically derived in the following two sub-Sections.

4.1. Maximum discharging energy (on-peak period)

During the *on-peak* period T^{on}, the maximum energy that is possible to be discharged by the battery can be derived by considering that the battery can be discharged only to supply the loads exceeding the RES power. More specifically, the maximum energy available for discharging, e^{dch}_{max}, is given by:

$$e^{dch}_{max} = \sum_{t\in T^{on}_{21}} \frac{1}{\eta_b}\left[\frac{p_{l,AC}(t)}{\eta_i} + p_{l,DC}(t) - p_r(t)\right]\Delta t + \sum_{t\in T^{on}_{22}} \frac{P_b}{\eta_b}\Delta t \tag{7}$$

where $p_{l,AC}(t)$ ($p_{l,DC}(t)$) is the power requested by the AC (DC) load at the time interval t, $p_r(t)$ is the power produced by the RES at the time interval t, P_b is the power rating of the battery, η_i is the efficiency of the converter between the AC and DC buses used as inverter, η_b is the battery efficiency, and where T^{on}_{21} and T^{on}_{22} are derived as follows.

As shown in Fig. 3, T^{on} includes two sub-periods (i.e., areas ① and ②) related to the RES power which is able (T^{on}_1) or not (T^{on}_2) to satisfy load demand:

$$\begin{aligned} T^{on}_1 &= \left\{t \in T^{on} : p_r(t) \geq \frac{p_{l,AC}(t)}{\eta_i} + p_{l,DC}(t)\right\} \\ T^{on}_2 &= \left\{t \in T^{on} : p_r(t) < \frac{p_{l,AC}(t)}{\eta_i} + p_{l,DC}(t)\right\} \end{aligned} \tag{8}$$

where t is the time slot of duration Δt.

During T^{on}_1 the RES power is able to satisfy the loads, thus the BESS is not requested to be discharged; during T^{on}_2 the BESS can be discharged to satisfy the loads exceeding the RES power, depending on the battery power rating, P_b. Thus, the following two sub-periods can be considered:

$$\begin{aligned} T^{on}_{21} &= \left\{t \in T^{on}_2 : \frac{p_{l,AC}(t)}{\eta_i} + p_{l,DC}(t) - p_r(t) \leq P_b\right\} \\ T^{on}_{22} &= \left\{t \in T^{on}_2 : \frac{p_{l,AC}(t)}{\eta_i} + p_{l,DC}(t) - p_r(t) > P_b\right\} \end{aligned} \tag{9}$$

4.2. Maximum charging energy (off-peak period)

During the off-peak periods T^{off}, the maximum charging energy of the battery can be derived by considering that the BESS can be charged from the RES power exceeding the loads first (i.e., area ⑤ in Fig. 3), and then by absorbing power from the grid (i.e., area ⑥ in Fig. 3). Particularly, the maximum energy that can be charged by the battery is given by:

$$e^{ch}_{max} = e^{r}_{T^{off}_1} + e^{r}_{T^{off}_2} + e^{g}_{T^{off}_2} \tag{10}$$

where, T^{off}_1 and T^{off}_2 are two subperiods of T^{off} referring to the case when RES power is able to satisfy the loads (T^{off}_1), or not (T^{off}_2); $e^{r}_{T^{off}_1}$ and $e^{r}_{T^{off}_2}$ are the maximum energies charged by the battery and supplied by the RES during the period T^{off}_1, and T^{off}_2, respectively and $e^{g}_{T^{off}_2}$ is the maximum energy that can be charged by the battery and that is supplied by the grid during T^{off}_2. These terms can be derived as explained in what follows.

T^{off}_1 and T^{off}_2 are given by:

$$\begin{aligned} T^{off}_1 &= \left\{t \in T^{off} : p_r(t) \geq \frac{p_{l,AC}(t)}{\eta_i} + p_{l,DC}(t)\right\} \\ T^{off}_2 &= \left\{t \in T^{off} : p_r(t) < \frac{p_{l,AC}(t)}{\eta_i} + p_{l,DC}(t)\right\} \end{aligned} \tag{11}$$

During T^{off}_1, the BESS can be charged by the RES power exceeding the loads, depending on the battery power rating, thus, it is possible to consider two sub-periods:

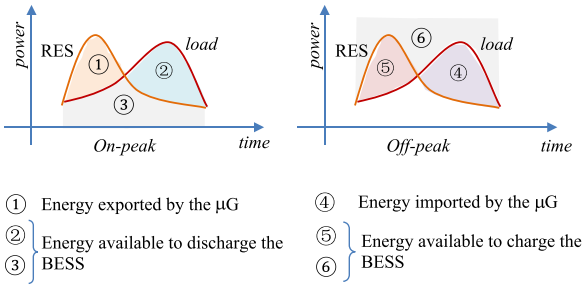

Fig. 3. Energy management strategy.

$$T_{11}^{off} = \left\{ t \in T_1^{off} : p_r(t) - \left[\frac{p_{l,AC}(t)}{\eta_i} + p_{l,DC}(t) \right] \geq P_b \right\}$$
$$T_{12}^{off} = \left\{ t \in T_1^{off} : p_r(t) - \left[\frac{p_{l,AC}(t)}{\eta_i} + p_{l,DC}(t) \right] < P_b \right\} \quad (12)$$

During the T_{11}^{off} and T_{12}^{off} the energy charged by the RES is given by:

$$e^r_{T_1^{off}} = \eta_b \sum_{t \in T_{11}^{off}} P_b \Delta t + \eta_b \sum_{t \in T_{12}^{off}} \left[p_r(t) - \left(\frac{p_{l,AC}(t)}{\eta_i} + p_{l,DC}(t) \right) \right] \Delta t \quad (13)$$

whereas the energy charged from the grid is zero.

During T_2^{off} the RES is not able to satisfy all the loads but only part or all of the DC loads; the power produced by the RES can then be used to charge the battery depending on the DC load request, thus identifying two sub-periods:

$$T_{21}^{off} = \left\{ t \in T_2^{off} : p_r(t) \geq p_{l,DC}(t) \right\}$$
$$T_{22}^{off} = \left\{ t \in T_2^{off} : p_r(t) < p_{l,DC}(t) \right\}. \quad (14)$$

During T_{21}^{off} the battery can be charged by both the grid and the RES depending on the battery power rating, P_b, thus identifying two sub-intervals:

$$T_{211}^{off} = \left\{ t \in T_{21}^{off} : p_r(t) - p_{l,DC}(t) \geq P_b \right\}$$
$$T_{212}^{off} = \left\{ t \in T_{21}^{off} : p_r(t) - p_{l,DC}(t) < P_b \right\}. \quad (15)$$

The maximum energy that can be charged by the battery during T_{21}^{off} from the RES, $e^r_{T_{21}^{off}}$, and from the grid, $e^g_{T_{21}^{off}}$, can be then evaluated as:

$$e^r_{T_{21}^{off}} = \eta_b \left[\sum_{t \in T_{211}^{off}} P_b + \sum_{t \in T_{212}^{off}} p_r(t) - p_{l,DC}(t) \right] \Delta t$$
$$e^g_{T_{21}^{off}} = \eta_b \left\{ \sum_{t \in T_{2121}^{off}} \left[P_b - \left(p_r(t) - p_{l,DC}(t) \right) \right] + \sum_{t \in T_{2122}^{off}} \eta_r \left[P_{imp}^{max} - p_{l,AC}(t) - \frac{\left(p_{l,DC}(t) - p_r(t) \right)}{\eta_r} \right] \right\} \Delta t \quad (16)$$

with η_r the efficiency of the converter between the AC and DC buses used as rectifier, and the intervals T_{2121}^{off} and T_{2122}^{off} defined on the basis of the maximum power that can be absorbed from the grid, P_{imp}^{max}, as:

$$T_{2121}^{off} = \left\{ t \in T_{212}^{off} : \frac{P_b - \left(p_r(t) - p_{l,DC}(t) \right)}{\eta_r} + p_{l,AC}(t) \leq P_{imp}^{max} \right\}$$
$$T_{2122}^{off} = \left\{ t \in T_{212}^{off} : \frac{P_b - \left(p_r(t) - p_{l,DC}(t) \right)}{\eta_r} + p_{l,AC}(t) > P_{imp}^{max} \right\}. \quad (17)$$

It is worth to note that a portion, $e^{g,AC}_{T_{21}^{off}}$, of $e^g_{T_{21}^{off}}$, is absorbed from the grid to supply part of the AC load which is given by:

$$e^{g,AC}_{T_{21}^{off}} = \eta_i \sum_{t \in T_{21}^{off}} \left[p_r(t) - p_{l,DC}(t) \right] \Delta t. \quad (18)$$

During T_{22}^{off} the battery can be charged by the grid, depending on the maximum power that can be absorbed, P_{imp}^{max}. Thus, two sub-periods can be defined within T_{22}^{off}:

$$T_{221}^{off} = \left\{ t \in T_{22}^{off} : p_{l,AC}(t) + \frac{P_b + p_{l,DC}(t) - p_r(t)}{\eta_r} > P_{imp}^{max} \right\}$$
$$T_{222}^{off} = \left\{ t \in T_{22}^{off} : p_{l,AC}(t) + \frac{P_b + p_{l,DC}(t) - p_r(t)}{\eta_r} \leq P_{imp}^{max} \right\}. \quad (19)$$

The maximum energy that can be charged by the battery during T_{22}^{off} can be then evaluated as:

$$e^g_{T_{22}^{off}} = \eta_b \left\{ \sum_{t \in T_{221}^{off}} \eta_r \left[P_{imp}^{max} - p_{l,AC}(t) - \frac{\left(p_{l,DC}(t) - p_r(t) \right)}{\eta_r} \right] + \sum_{t \in T_{222}^{off}} \frac{P_b}{\eta_r} \right\} \Delta t. \quad (20)$$

The maximum energy that can be charged by the battery from the RES, $e^r_{T_2^{off}}$, and from the grid, $e^g_{T_2^{off}}$ are eventually given by:

$$e^r_{T_2^{off}} = e^r_{T_{21}^{off}}$$
$$e^g_{T_2^{off}} = e^g_{T_{21}^{off}} + e^g_{T_{22}^{off}}. \quad (21)$$

In the case of three-level ToU tariff, a mid-peak period can be considered where the battery can also be charged with the same procedure presented for the *off-peak* period.

4.3. Energy exchanges during the on-peak period

As previously evidenced, in order to analytically evaluate the cost and revenue items in (4) and (5), the sold and purchased energy have to be evaluated. In this sub-section, these terms are derived with respect to the *on-peak* period. Particularly, the energy sold during the *on-peak* period, $E^{sT^{on}}$, is that corresponding to the RES power exceeding the load, during the T_1^{on}, that is when the RES production is higher than the load, and has the same value independently from the presence or absence of the BESS

$$E^{sT^{on}} = \sum_{t \in T_1^{on}} \left[\eta_i \left(p_r(t) - p_{l,DC}(t) \right) - p_{l,AC}(t) \right] \Delta t. \quad (22)$$

During T_2^{on}, when the RES production is lower than the load, the sold energy is zero.

Regarding the energy purchased during the *on-peak* period, $E^{pT^{on}}$, in the case of absence of BESS, during the interval T_1^{on} when the RES production is higher than the load, it is equal to zero. It is different from zero only when the RES production is lower than the load (i.e., T_2^{on}) and is given by:

$$E^{pT^{on}}_{nobs} = \sum_{t \in T_2^{on}} \left[p_{l,AC}(t) - p_{r,AC}(t) + \frac{p_{l,DC}(t) - p_{r,DC}(t)}{\eta_r} \right] \Delta t \quad (23)$$

where $p_{r,AC}(t)$ and $p_{r,DC}(t)$ are the portions of the RES production used to supply AC and DC loads, respectively, which are given by:

$$p_{r,DC}(t) = \begin{cases} p_{l,DC}(t) & p_r(t) \geq p_{l,DC}(t) \\ p_r(t) & otherwise \end{cases} \quad (24)$$

$$p_{r,AC}(t) = \begin{cases} p_{l,AC}(t) & \eta_i\left(p_r(t) - p_{r,DC}(t)\right) \geq p_{l,AC}(t) \\ \left[p_r(t) - p_{r,DC}(t)\right]\eta_i & otherwise. \end{cases} \quad (25)$$

In the case of presence of BESS, the purchased energy, $E^{pT^{on}}$, is obtained, starting from (23), as:

$$E^{pT^{on}} = E^{pT^{on}}_{nobs} - \eta_b e^{T^{on}}_{DC} - \eta_b \eta_i e^{T^{on}}_{AC} \quad (26)$$

where $e^{T^{on}}_{DC}$ ($e^{T^{on}}_{AC}$) is the energy discharged by the battery to satisfy the DC (AC) load. Being e the whole energy discharged by the battery, $e^{T^{on}}_{DC}$ and $e^{T^{on}}_{AC}$ are given by:

$$e^{T^{on}}_{DC} = \begin{cases} \sum_{t\in T^{on}_2}\left[p_{l,DC}(t) - p_r(t)\right]\Delta t & \eta_b e \geq \sum_{t\in T^{on}_2} p_{l,DC}(t)\Delta t \\ e & otherwise \end{cases} \quad (27)$$

$$e^{T^{on}}_{AC} = \begin{cases} e - e^{T^{on}}_{DC} & \eta_b e \geq \sum_{t\in T^{on}_2} p_{l,DC}(t)\Delta t \\ 0 & otherwise. \end{cases} \quad (28)$$

4.4. Energy exchanges during the off-peak period

Regarding the *off-peak* period, T^{off}, the battery is supposed to be charged by the RES production which exceeds the loads, first, then by the energy supplied by the grid.

During this period, since during the T^{off}_2, i.e., when the RES production is lower than the load, the sold energy is zero, the energy is sold only during the T^{off}_1, i.e., when the RES production exceeds the load. Thus, in absence of BESS, the sold energy ($E^{sT^{off}}_{nobs}$) is given by:

$$E^{sT^{off}}_{nobs} = \sum_{t\in T^{off}_1}\left[\eta_i\left(p_r(t) - p_{r,DC}(t)\right) - p_{r,AC}(t)\right]\Delta t. \quad (29)$$

In the case of the presence of BESS, the RES power exceeding the load demand is used to charge the battery and, that exceeding both loads and battery power rating is sold to the upstream grid. Thus, the sold energy, $E^{sT^{off}}$, is given by:

$$E^{sT^{off}} = \begin{cases} E^{sT^{off}}_{nobs} - \dfrac{\eta_i}{\eta_b} e & e \leq e^r_{T^{off}_1} \\ E^{sT^{off}}_{nobs} - \dfrac{\eta_i}{\eta_b} e^r_{T^{off}_1} & otherwise \end{cases} \quad (30)$$

where $e^r_{T^{off}_1}$, given by (13), is the energy corresponding to the portion of power produced by the RES and used to charge the battery.

Regarding the purchased energy in absence of BESS, $E^{pur,T^{off}}_{nobs}$, it is equal to zero during T^{off}_1 whereas, during T^{off}_2, i.e., when the RES production is lower than the load, it is given by:

$$E^{pT^{off}}_{nobs} = \sum_{t\in T^{off}_2}\left[p_{l,AC}(t) - p_{r,AC}(t) + \frac{p_{l,DC}(t) - p_{r,DC}(t)}{\eta_r}\right]\Delta t \quad (31)$$

where $p_{r,AC}(t)$ and $p_{r,DC}(t)$ are still given by (24) and (25).

In the case of presence of BESS, the battery is charged by the grid during T^{off}_2, i.e., when the RES production is lower than the load demand. Thus, the purchased energy during T^{off}, $E^{pT^{off}}$, is given by:

$$E^{pT^{off}} = \begin{cases} E^{pT^{off}}_{noB} & e \leq e^r_{T^{off}_1} \\ E^{pT^{off}}_{noB} + \dfrac{1}{\eta_r\eta_b}\left(e - e^r_{T^{off}_1}\right) & e^r_{T^{off}_1} < e \leq e_1 \\ E^{pT^{off}}_{noB} + \dfrac{1}{\eta_r\eta_b} e^g_{T^{off}_{22}} + \eta_i(e - e_1) & e_1 < e \leq e_2 \\ E^{pT^{off}}_{noB} + \dfrac{1}{\eta_r\eta_b}\left[e^g_{T^{off}_{22}} + (e - e_2)\right] + \eta_i e^{g,AC}_{T^{off}_{21}} & otherwise \end{cases} \quad (32)$$

where $e_1 = e^g_{T^{off}_{22}} + e^r_{T^{off}_1}$ and $e_2 = e^g_{T^{off}_{22}} + e^r_{T^{off}_1} + e^{g,AC}_{T^{off}_{21}}$.

Note that in the first equation of (32), the BESS energy overall charged and discharged is lower than or equal to that available from the RES. It means that no energy is purchased from the grid to charge the BESS and the energy purchased from the grid is solely that required by the load, that is the same of the case of absence of BESS.

5. Taguchi Arrays-Based probabilistic procedure

5.1. The Taguchi method and the orthogonal arrays

The Taguchi method is a statistical method belonging to the design of experiment techniques, which are typically adopted to study the effect of multiple variables on the output [19]. These techniques manage statistical processes by identifying:

(i) the *system*, described by the equation governing the problem under study;
(ii) *inputs*, which are data used to run the problem;
(iii) *outputs*, which are the responses of the system;
(iv) *factors*, which are data that have a direct effect on the outputs; each factor can assume different values referred to as *levels*;
(v) *uncontrollable noises*, which are variables that affect the outputs but whose values are unidentifiable [27].

The design of experiment techniques deals with all the possible levels associated with the factors. From a theoretical point of view, their effect on the outputs should be identified by the analysis of the experiments applied to all possible combinations of all factor levels. This would imply a huge number of experiments, N_{exp}, which corresponds to $N_{exp} = N_L^{N_F}$, being N_F the number of factors and N_L the number of levels, with obvious huge computational burden.

The Taguchi method is based on orthogonal *arrays*, as that shown in Table 1, which allow identifying the fewest possible experiments to be performed which correspond to a specified combination of the levels of factors. In particular, the orthogonal array is a matrix that individuates the fewest fraction of the exhaustive factorial combinations N_{exp} having the property to adequately represent the impact of the factor randomness on the outputs. These orthogonal arrays have a number of columns equal to the number of factors N_F and a number of rows referring to the number of experiments $N_{exp,T}$; considering the i^{th} row and the j^{th} column, the element L_{ij} is the level assigned to the j^{th} factor in the i^{th} experiment (e.g., L_{ij} can be 1 or 2, in case of factors with two levels; 1, 2 and 3 in case of three levels) [19,28]. The properties of the orthogonal arrays are widely explained in [19].

Table 1
Example of orthogonal array.

Experiment number	Level of each factor			
	F_1	F_2	….	F_{N_F}
1	L_{11}	L_{12}	…	L_{1N_F}
2	L_{21}	L_{22}	…	L_{2N_F}
….	…	…	…	…
$N_{exp,T}$	$L_{N_{exp,T}1}$	$L_{N_{exp,T}2}$	…	$L_{N_{exp,T}N_F}$

The combination of factor levels of each experiment of the orthogonal arrays can be derived, based on specific rules, by using libraries [35] and/or algorithms [36]. To provide an example of the determination of the orthogonal arrays, let us consider the orthogonal array for a case with 3 factors that can assume two levels; as reported in Table 2, where the two levels assigned to each factor are indicated by 1 and 2, the number of rows (and of the experiments) is only 4.

The orthogonal arrays exhibit some properties [19]: first, each column of the array contains the same number of the levels (e.g., the first column of Table 2 contains twice the level 1 and twice the level 2, and so on); second, the combinations of factors' levels between any two columns appear an equal number of times (e.g., in Table 2, the combinations of the levels 1 and 2 for the factors F_1, F_2, and F_3 − 11, 22, 21, and 12 - appear in the corresponding columns.) The minimum number of rows that verifies the mentioned rules is the number of Taguchi's orthogonal array.

By applying the Taguchi's orthogonal arrays, the number of experiments, $N_{exp,T}$, is such that the number of columns of the orthogonal matrix $N_{F^*} = \frac{(N_L{}^J - 1)}{(N_L - 1)}$ is greater than or equal to the number of factors, N_F, where J is selected such that the number of experiments $N_{exp,T} = N_L{}^J$, which corresponds to the number of rows of the orthogonal matrix. In case N_{F^*} is greater than the number of factors N_F, the redundant columns can be neglected, since the obtained array is still orthogonal [36]. It is easy to argue, that the number of experiments of the Taguchi's orthogonal arrays, $N_{exp,T}$, is significantly lower than the number of experiments corresponding to all the combinations N_{exp}.

Regarding the levels of the factors, the Taguchi orthogonal arrays usually refer to two or three levels.

A factor can be also represented by a random variable with an assigned pdf (as in the case of the probabilistic sizing of BESS). In this case, the orthogonal arrays can still be derived by assigning two or three levels to the factors in agreement with the assigned pdfs; in particular, for a two-level array, the values associated with the levels of the i^{th} random variable (factor) can be chosen as [27]:

$$\mu_i \mp \sigma_i \tag{33}$$

where μ_i and σ_i are the mean and the standard deviation values, respectively, of the i^{th} random variable (factor).

When a three-level array is chosen, the values associated with the levels of the i^{th} random variable (factor) are μ_i and

$$\mu_i \mp \sqrt{\frac{3}{2}}\sigma_i. \tag{34}$$

The outputs of the procedure are the mean and standard deviation values of the results of all the experiments [28]. In this paper, the orthogonal arrays are used to create the possible set of experiments which allow handling uncertainties of the input parameters of the sizing procedure and obtaining the probabilistic features of the candidate BESS sizes in terms of mean and standard deviation of the total cost. In this way, the use of Taguchi orthogonal arrays allows managing the large set of uncertain parameters involved in the sizing procedure, through a small number of experiments even preserving the accuracy of typical probabilistic approaches based on a large number of experiments, such as the Monte Carlo method. The application of the Taguchi arrays to the sizing procure is detailed in Section 5.2.

Table 2
Orthogonal array for 3 factors and 2 levels [19].

Experiment number	Level of each factor		
	F_1	F_2	F_3
1	1	1	1
2	1	2	2
3	2	1	2
4	2	2	1

5.2. Application of Taguchi arrays to the sizing procedure

For each BESS size, the total cost (as formulated in Sections 3 and 4) depends on input variables or data that are uncertain and, as a consequence, is itself a random variable. To determine the statistical properties of the sizing objective, a variety of methods can be applied; among them the well-known Monte Carlo simulation procedure, which is one of the most used techniques, can be implemented. However, since this method suffers from a huge computational burden, lately, approximate approaches have been proposed to face problems under uncertainties with lower computational efforts [37]. In this paper, the Taguchi method is chosen and, for all the elements of the orthogonal array determined for the factors (the factors being random input data of the optimization problem), the analytical problem explained in Sections 3 and 4 is applied and, in the end, the statistical measures of the sizing objective are determined.

More specifically, referring to the flow chart of Fig. 4 and to the hybrid μG described in Section 2, the input data are the maximum power which can be exchanged between the μG and the main grid, the structure of the energy tariff, and the possible sizes of the BESS among which the optimal value must be identified. The random variables (i.e., factors according to Taguchi's nomenclature) of the proposed sizing procedure are:

(i) the price of the purchased energy,
(ii) the price of the sold energy,
(iii) the load demand, and
(iv) the PV power.

Statistical distributions are identified for each random variable, according to the available data. After determining the proper orthogonal array (on the basis on the chosen number of levels, e.g. two-level or three-level approach), for each element belonging to it, the total costs

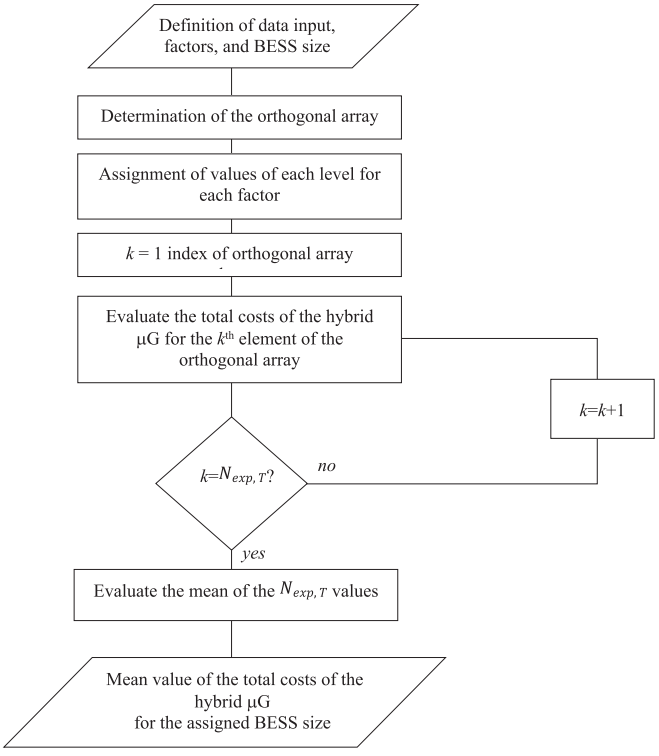

Fig. 4. Schematic representation of the application of the Taguchi's arrays for an assigned BESS size.

are determined by applying the analytical formulation described in Sections 3 and 4. Outputs are the mean values of the total cost of the μG over the whole planning period corresponding to the considered BESS size.

The procedure of Fig. 4 has to be applied to all the available BESS sizes and, finally, the optimal BESS size will be the one associated to the lowest mean value of the total cost of the μG.

It is worth noting that, in the numerical applications, for some cases, the Monte Carlo method is reported to test the effectiveness and the accuracy of the Taguchi arrays-based method; for the Monte Carlo method, a few thousands of simulations are required.

6. Numerical application

The proposed planning method has been applied to the hybrid μG of an industrial load characterized by both AC and DC power demand and equipped with a PV system. The classic Monte Carlo approach, which is a benchmark method widely used in scientific community [37], is used to validate the proposed method. The power demand has been considered based on the historical measurements of 50 actual industrial plants in Germany [38]. Pre-processing has been performed related to the values originally collected at a minute resolution which have been averaged to obtain hourly data. Also, based on the available one-year historical data, pdfs are derived with reference to four typical days, corresponding to working/holiday and summer/winter. Mean and standard deviation values of the pdfs are derived for the application of the Taguchi arrays-based method. Two examples of summer and winter AC and DC loads data are reported in Fig. 5(a) and (b).

A five MW-rated photovoltaic (PV) system has also been considered. The historical values of its power production were adapted from [39]. In Fig. 5(c), two examples of daily PV production are reported, related to a winter and summer day.

Data related to the load and PV powers are already available pre-processed, thus no issues related to missing or bad data have been faced with. The data of each experiment of the probabilistic procedure, which are supposed uncorrelated, are extracted from the non-parametric distributions of loads and PV hourly powers.

A yearly load growth of + 1 % has been assumed for both AC and DC loads. Regarding the ToU tariff, the prices assumed for the first year are reported in Table 3. They refer to an actual tariff applied to industrial

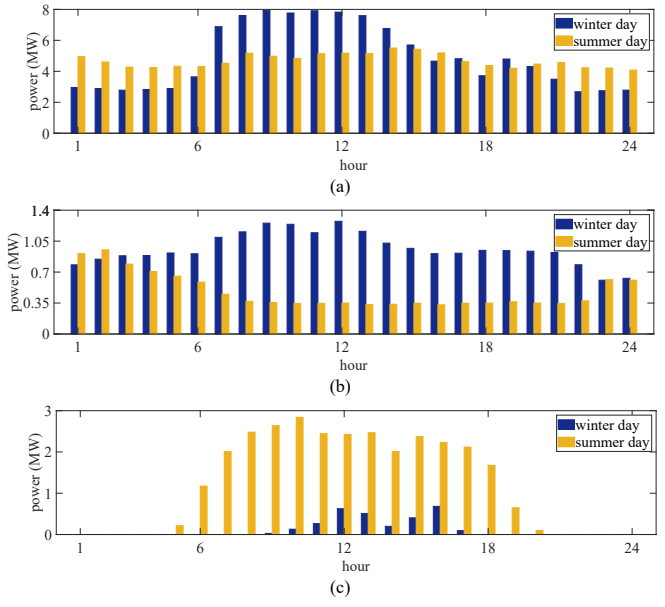

Fig. 5. Examples of AC load demand (a), DC load demand (b), and PV production (c).

Table 3
ToU Tariff.

Season	TOU level	Period	Price ($/MWh)
Summer tariff	On peak	4p.m. to 9p.m.	388.73
	Mid Peak	2p.m. to 4p.m. 9p.m. to 11p.m.	213.99
	Off Peak	*all other hours*	156.94
Winter tariff	On peak	4p.m. to 9p.m.	177.35
	Off Peak	*all other hours*	139.70

loads equipped with energy storage systems available from [40].

Regarding the feed-in tariff, based on the actual rates provided by the same utility, the price of 50 $/MWh has been assumed for the first year according to the tariff available from [40]. During the planning period the values of both feed-in and ToU tariffs vary according to a uniform distribution with mean, μ, equal to the value of the tariff and parameters $\mu \pm 10\%$. A yearly growth of 1 % has also been assumed. The net present value of the total cost is obtained by considering the discount rate of 3 %.

The storage device is based on the nickel manganese cobalt Li-ion battery technology. For this technology, the round-trip efficiency is 99 %, the discharging time is three hours, and the maximum admissible DoD is 100 %, corresponding to a lifetime of 4800 cycles [41]. The battery's installation and replacement costs are assumed equal to 153 and 110 $/kWh, respectively; the installation cost of the conversion system is assumed equal to 59.6 $/kW; maintenance costs of 1.5 % of the installation cost are assumed for the BESS [41]. The proposed sizing tool is applied with respect to a planning time of 20 years.

In this case study, the number of factors is 241; if we consider two levels for each factor, the Taguchi's orthogonal array will contain 256 rows (experiments), while for the 3-level case, the Taguchi's orthogonal array will contain 729 rows (experiments). The orthogonal arrays are determined, on the basis of the previously mentioned properties, by applying the algorithm described in [36]. With respect to the values assumed by the random factors, for the 2-level approach, (33) provides the values of each factor, while for the 3-level approach, the values of the factors are the mean and the values provided by (34). Regarding the computational time, the use of Taguchi two-level implies less than 0.1 s for the evaluation of mean and standard deviation of the total cost for each size, based on the simulation performed with a PC equipped with an Intel(R) Core(TM) i9-10900X CPU @ 3.70 GHz – 64 GB RAM. Obviously, in this application the reduced computational time is due to the use of an analytical procedure. The computational time quantified with the Taguchi three-level was about seven times longer than that of the Taguchi two-level. The computational time quantified with the Monte Carlo method was about 40 times longer than that of the Taguchi two-level. Hence, significant time reduction can be attained when dealing with a large set of BESS sizes among which the solution would be found.

The mean values of the total costs resulting from the application of the proposed method are reported in Fig. 6 with respect to BESS sizes

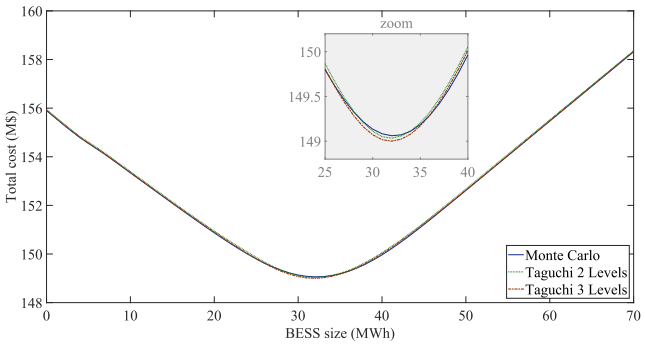

Fig. 6. Total cost for different BESS sizes.

ranging in the interval 0 – 70 MWh. For comparative purposes, in Fig. 6 the results of the application of the Monte Carlo method, of the 2-level Taguchi arrays approach, and of the 3-level Taguchi arrays approach are shown. As it clearly appears in the figure, the three probabilistic approaches give very similar results. Indeed, the BESS size corresponding to the minimum total costs is 32 MWh in all the cases. The costs sustained by adopting this BESS size are very similar independently of the adopted probabilistic method. The negligible difference in these results demonstrates the accuracy of the proposed approach despite a noticeably lower number of experiments.

In Tables 4 and 5 the results of other comparisons of Monte Carlo and Taguchi 2-level based-methods are reported with respect to different PV ratings and DC load requests. Regarding the results of the Taguchi 3-level based-method, they are very similar to those obtained by applying the 2-level based-method, thus they are not reported.

The effect of the PV power rating is shown in Table 4, where the total costs are reported for the cases of no PV systems, 5 MW (base PV) and 10 MW (increased PV) rated power. As expected, the total cost reduces and the BESS optimal size decreases with the increase of the PV rated power. The differences between the results obtained with the Taguchi-based and Monte Carlo-based approaches are negligible.

In Table 5 the above results related to the base DC (hereinafter referred to as base DC) are reported together with other results obtained with the other two different DC load requests, namely, no DC load, and increased DC load (double of the DC load value of the base case). Note that, in all the three cases, the whole load (AC and DC) is constant, which means that, compared to the case of base DC load, an increased AC load is considered in case of no DC load, and a reduced AC load is considered in the case of increased DC load.

The results in Table 5 clearly show that, in the considered case studies, the optimal size of the BESS is not affected by the ratio of DC load/AC load. This ratio, however, has some not negligible effects on the total cost corresponding to the optimal battery size, which slightly decreases for increasing DC load. This is due to the fact that with the increase of DC load, the losses due to the conversion stage are reduced. The results of Table 5 also demonstrate, again, that the differences between the results obtained with the Taguchi-based and Monte Carlo-based approaches are negligible, so still demonstrating the validity and accuracy of the proposed approach.

As further examples, some results of the proposed method are reported with respect to different values of yearly increments of load and energy price ranging from zero to 5 %. The results are reported in Fig. 7 (load growth variations) and Fig. 8 (price growth variations) which, for clarity purposes, refer to the 2-level Taguchi method; the results are reported in relative values with reference to the case without the BESS.

The results shown in Fig. 7 clearly show that larger yearly load increments imply larger BESS sizes and lower total cost reduction. In particular, as the increments increase from zero to 5 %, BESS sizes increase from 29 MWh to 45 MWh and the cost reduction decreases from about 5 % to 4 %. In the case of larger values of yearly energy price increments (Fig. 8), larger cost reduction appears by using BESS. As a consequence, larger values of the BESS optimal size are obtained. In this case, as the increments vary from zero to 5 %, the BESS size slightly increases from 31 MWh to 35 MWh and the cost reduction increases from about 4 % to about 7 %. This is coherent with the proposed BESS management, which allows increasing the economic advantages as the energy price increases. Note that, in this application, benefits other than economical have not been considered. The use of the BESS in power systems, indeed, has a significant impact in terms of demand response or self-consumption increase and then, in terms of environmental benefits and efficient operation. This would have further increased the overall advantages the BESS can provide.

Other simulations have been performed by applying 3-level Taguchi and Monte Carlo methods. In all the cases the differences with respect to the results of the 2-level Taguchi method are still negligible. Further simulations were performed to analyse also the cost reduction obtained by applying a “whole-year operation strategy” and a “summer operation strategy”. The former refers to the use of the BESS for the entire year, whereas the latter refers to the use of BESS only in the summer periods which are typically characterized by larger on/off-peak price variations. As shown in [42] the summer strategy can allow reducing the costs thanks to the reduced use of the BESS so avoiding replacement costs. The results are shown in Fig. 9 where the total costs resulting from the application of the two strategies are reported for different BESS sizes.

By analysing Fig. 9, it clearly appears that, in the case of the summer strategy, the total costs are always lower than those of the whole-year operation strategy. It also appears that the difference between the two curves increases as the BESS size increases. The optimal BESS size in the case of summer strategy is 33 MWh, which is slightly larger than that corresponding to the whole year operation. The corresponding

Table 4
Optimal battery size and corresponding total cost for different PV ratings.

PV option method	no PV	base PV	increased PV
Monte Carlo	37 MWh (164.09 M$)	32 MWh (149.33 M$)	27 MWh (136.39 M$)
2-Level Taguchi	37 MWh (164.08 M$)	32 MWh (148.99 M$)	27 MWh (136.70 M$)

Table 5
Optimal battery size and corresponding total cost for different DC load ratings.

DC load option method	no DC	base DC	increased DC
Monte Carlo	32 MWh (151.86 M$)	32 MWh (149.33 M$)	32 MWh (148.97 M$)
2-Level Taguchi	32 MWh (151.89 M$)	32 MWh (148.99 M$)	32 MWh (149.00 M$)

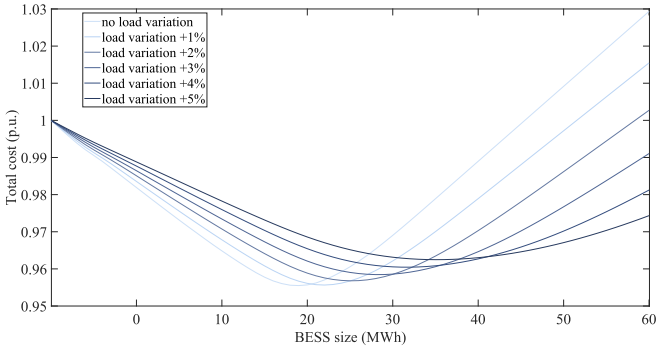

Fig. 7. Total cost for different BESS sizes and various yearly load increments.

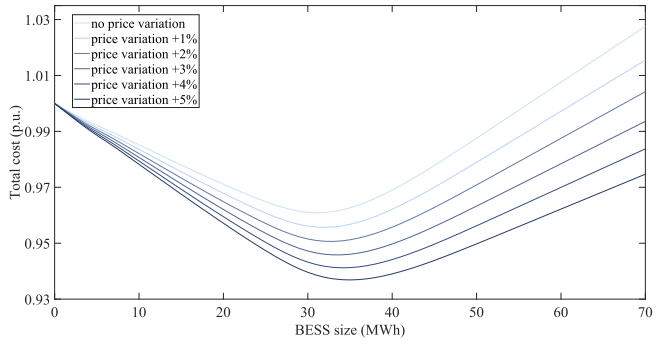

Fig. 8. Total cost for different BESS sizes and various yearly energy price increments.

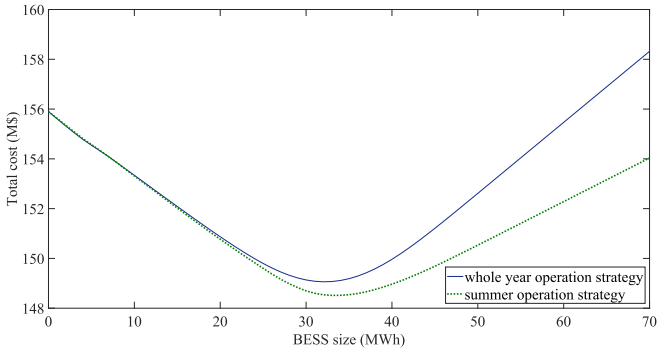

Fig. 9. Total cost for different BESS sizes with whole year and summer operation strategies.

minimum cost is 148.52 M$, which is slightly lower than that obtained in the case of the whole year operation strategy (i.e., less than 1 %).

The results of the considered case studies confirm the feasibility of the proposed tool. With reference to the dependence of the optimal size of the BESS from the design parameters, the analysis of the results suggested that larger RES ratings correspond to smaller BESS sizes while the BESS size does not vary with the DC load rating, even if an impact on the total costs has been recognized. More significant impact has the annual variation of the total load demand, since larger BESS sizes are identified when greater annual increase rates are assumed. Similarly, greater annual price variation implies larger BESS sizes.

7. Conclusion

The widespread use of μGs with AC and DC sections along with the diffusion of renewable power generation require the installation of BESSs in order to optimally manage the resources and to reduce the operating costs. However, when determining the optimal size of the BESS, some uncertainties have to be considered.

In this paper, a procedure to optimally size a BESS in hybrid μGs was proposed which accounts for uncertainties in load demand, renewable power generation and electricity prices. The sizing procedure is based on the evaluation of the total costs in a μG including a BESS, AC and DC loads and renewable generation and on an analytical formulation for the management of the BESS to determine the daily charging/discharging profile. The uncertainty has been handled by means of the Taguchi arrays which allows taking into consideration different combinations of the uncertain input parameters while reducing the number of experiments needed to consider their randomness.

A case study including an industrial customer with AC and DC loads and photovoltaic generation was examined. The feasibility of the proposed tool was demonstrated and the comparison with the results obtained by means of the Monte Carlo method confirmed the accuracy of the proposed approach in spite of the reduced computational burden. The dependence between some input parameters and the optimal size of the BESS was investigated; for instance, larger photovoltaic ratings correspond to smaller BESS sizes coherently with the main purpose of the strategy that is the provision of demand response. It has to be noted that, in the cost analysis, benefits other than economical, such as environmental, could be considered since they are significant for sustainable development of power systems. This would have further increased the overall advantages the BESS can provide. The use of BESS in power systems, indeed, has a significant impact in terms of demand response or self-consumption increase and, then, in terms of environmental benefits and efficient operation.

The main findings of the paper are:

- the deployment of the analytical formulation of the management problem of the BESS together with the Taguchi's approach to account for uncertainties reduces the computational burden for the optimal sizing of the BESS in a hybrid μG while guaranteeing adequate levels of accuracy in the determination of the optimal solution.
- the optimal sizing of the BESS allows the industrial customer to reduce the costs over the considered period.
- the optimal sizing of the BESS depends also on its management strategy; numerical results gave evidence that the "summer operation strategy" (i.e., the use of the storage system only in the summer periods characterized by higher electrical energy costs) is associated to a further cost reduction.

Future research will be devoted to the application of further probabilistic approximate methods to evaluate the statistical properties of the total cost of the hybrid μG and to consider further renewable plants.

CRediT authorship contribution statement

Fabio Mottola: Conceptualization, Data curation, Formal analysis, Investigation, Methodology, Software, Validation, Writing – original draft, Writing – review & editing. **Daniela Proto:** Conceptualization, Data curation, Formal analysis, Investigation, Methodology, Software, Validation, Writing – original draft, Writing – review & editing. **Angela Russo:** Conceptualization, Data curation, Formal analysis, Investigation, Methodology, Software, Validation, Writing – original draft, Writing – review & editing.

Declaration of competing interest

The authors declare that they have no known competing financial interests or personal relationships that could have appeared to influence the work reported in this paper.

Data availability

The source of data are cited in the paper.

Acknowledgements

The authors thank Prof. Guido Carpinelli who provided insights and expertise that greatly assisted this research.

References

[1] Hannan MA, et al. Review of optimal methods and algorithms for sizing energy storage systems to achieve decarbonization in microgrid applications. Renew Sustain Energy Rev 2020;131:110022.
[2] Yan C, Geng X, Bie Z, Xie L. Two-stage robust energy storage planning with probabilistic guarantees: a data-driven approach. Appl Energy 2022;313:118623.
[3] Carpinelli G, Mottola F, Proto D. Probabilistic sizing of battery energy storage when time-of-use pricing is applied. Electr Power Syst Res 2016;141:73–83.
[4] Abdulgalil MA, Khalid M, Alismail F. Optimal sizing of battery energy storage for a grid-connected microgrid subjected to wind uncertainties. Energies 2019;12:2412.
[5] Garmabdari R, Moghimi M, Yang F, Gray E, Lu J. Multi-objective energy storage capacity optimisation considering microgrid generation uncertainties. Int J Electr Power Energy Syst 2020;119:105908.
[6] Sedghi M, Ahmadian A, Aliakbar-Golkar M. Optimal storage planning in active distribution network considering uncertainty of wind power distributed generation. IEEE Trans Power Syst 2016;31(1):304–16.
[7] Delgado-Antillón CP, Domínguez-Navarro JA. Probabilistic siting and sizing of energy storage systems in distribution power systems based on the islanding feature. Electr Power Syst Res 2018;155:225–35.
[8] Bucciarelli M, Paoletti S, Vicino A. Optimal sizing of energy storage systems under uncertain demand and generation. *Appl Energy* 2018;225:611–21.
[9] Bracale A, Caramia P, Mottola F, Carpinelli G, Proto D. Probabilistic sizing of battery energy storage system in presence of renewable generation. *IEEE int. conf. on prob. methods appl. to*. Power 2018. Syst. (PMAPS),.
[10] Bludszuweit H, Domínguez-Navarro JA. A probabilistic method for energy storage sizing based on wind power forecast uncertainty. IEEE Trans Power Syst 2011;26 (3):1651–8.

[11] Wu J, Zhang B, Li H, Li Z, Chen Y, Miao X. Statistical distribution for wind power forecast error and its application to determine optimal size of energy storage system. Int J Electr Power Energy Syst 2014;55:100–7.
[12] Michiorri A, Lugaro J, Siebert N, Girard R, Kariniotakis G. Storage sizing for grid connected hybrid wind and storage power plants taking into account forecast errors autocorrelation. Renew Energy 2018;117:380–92.
[13] Wang C, Liang Z, Liang J, Teng Q, Dong X, Wang Z. Modeling the temporal correlation of hourly day-ahead short-term wind power forecast error for optimal sizing energy storage system. Int J Electr Power Energy Syst 2018;98:373–81.
[14] Xia S, Chan KW, Luo X, Bu S, Ding Z, Zhou B. Optimal sizing of energy storage system and its cost-benefit analysis for power grid planning with intermittent wind generation. Renew Energy 2018;122:472–86.
[15] Yan C, Geng X, Xie L, Bie Z. A scenario-based storage planning framework with probabilistic guarantees. IEEE Sustainable Power and Energy Conference (iSPEC) 2019.
[16] Nayeem C, Pilo F, Pisano G. Optimal energy storage system positioning and sizing with robust optimization. Energies 2020;13:512.
[17] Akhavan-Hejazi H, Mohsenian-Rad H. Energy storage planning in active distribution grids: a chance-constrained optimization with non-parametric probability functions. IEEE Trans Smart Grid 2018;9(3):1972–85.
[18] Ntube N, Li H. Stochastic multi-objective optimal sizing of battery energy storage system for a residential home. J Storage Mater 2023;59:106403.
[19] Roy RK. Design of experiments using the Taguchi approach. New York: John Wiley & Sons Inc.; 2001.
[20] Liu D, Cai Y. Taguchi method for solving the economic dispatch problem with nonsmooth cost functions. IEEE Trans Power Syst 2005;20(4):2006–14.
[21] Lin WM, Gowa HJ, Tsai MT. An efficient hybrid Taguchi-immune algorithm for the unit commitment problem. Int J Expert Syst Appl 2011;38(11):13662–9.
[22] Yu H, Chung CY, Wong KP. Robust transmission network expansion planning method with Taguchi's orthogonal array testing. IEEE Trans Power Syst 2011;26 (3):1573–80.
[23] Subbaraj P, Rengaraj R, Salivahanan S. Enhancement of self-adaptive real coded genetic algorithm using taguchi method for economic dispatch problem. Appl Soft Comput 2011;11(1):83–9.
[24] Yu H, Rosehart WD. An optimal power flow algorithm to achieve robust operation considering load and renewable generation uncertainties. IEEE Trans Power Syst 2012;27(4):1808–17.
[25] Hasanien HM. Design optimization of PID controller in automatic voltage regulator system using taguchi combined genetic algorithm method. IEEE Syst J 2013;7(4): 825–31.
[26] Basetti V, Chandel AK. Hybrid power system state estimation using taguchi differential evolution algorithm. IET Sci Meas Technol 2015;9(4):449–66.
[27] Hong YY, Lin FJ, Yu TH. Taguchi method-based probabilistic load flow studies considering uncertain renewables and loads. IET Renew Power Gener 2016; **10**: 221-227.
[28] Carpinelli G, Rizzo R, Caramia P, Varilone P. Taguchi's method for probabilistic three-phase power flow of unbalanced distribution systems with correlated wind and photovoltaic generation systems. Renew Energy 2018;117:227–41.
[29] Meena NK, et al. Modified taguchi-based approach for optimal distributed generation mix in distribution networks. IEEE Access 2019;7:135689–702.
[30] Zeinal-Kheiri S, Shotorbani AM, Mohammadi-Ivatloo B. Robust energy management of a microgrid with uncertain price, renewable generation, and load using taguchi's orthogonal array method. J Energy Technol Res 2019;3(3):1–13.
[31] Hong Y-Y, Nguyen M-T. Multiobjective multiscenario under-frequency load shedding in a standalone power system. IEEE Syst J 2020;14(2):2759–69.
[32] Reza Nikzad H, Abdi H. A robust unit commitment based on GA-PL strategy by applying TOAT and considering emission costs and energy storage systems. Electr Power Syst Res 2020;180:106154.
[33] Najjarpour M, Tousi B, Jamali S. Loss reduction in distribution networks with DG units by correlating taguchi method and genetic algorithm. Iran J Electr Electron Eng 2022;18(4):2429.
[34] Unamuno E, Andoni BJ. Hybrid ac/dc microgrids—Part I: review and classification of topologies. Renew and Sust Energy Reviews 2015;52:1251–9.
[35] Orthogonal Arrays (Taguchi Designs). [Online]. Available: http://www.york.ac.uk/depts/maths/tables/orthogonal.htm.
[36] Leung YW, Wang Y. An orthogonal genetic algorithm with quantization for global numerical optimization. IEEE Trans Evol Comput 2001;5(1):41–53.
[37] Prusty BR, Jena D. A critical review on probabilistic load flow studies in uncertainty constrained power systems with photovoltaic generation and a new approach. Renew Sustain Energy Rev 2017;69:1286–302.
[38] Braeuer F, Rominger J, McKenna R, Fichtner W. Battery storage systems: an economic model-based analysis of parallel revenue streams and general implications for industry. App Energy 2019;239:1424–40.
[39] Raouf Mohamed AA, Best R, Liu X, Morrow J. One-year half-hourly profiles of demand, PV generation, and EV charging for a household in London, UK. IEEE Dataport [Online] Available: https://dx.doi.org/10.21227/8vhr-2572.
[40] Rates—Pacific gas and electric company. [Online] Available from http://www.pge.com/tariffs/.
[41] Electricity Storage and Renewables: Costs and Markets to 2030, International Renewable Energy Agency, Abu Dhabi. [Online]. Available http://www.irena.org/publications/2017/Oct/Electricity-storage-and-renewables-costs-and-markets.
[42] Carpinelli G, Mottola F, Noce C, Russo A, Varilone P. A new hybrid approach using the simultaneous perturbation stochastic approximation method for the optimal allocation of electrical energy storage systems. Energies 2018;11:1505.